DOI: 10.4149/BLL_2023_051

Bratisl Med J

Alzheimer' disease prediction and classification using CT images through machine learning

Raveendra REDDY, Rama KRISHNA

Department of Computer Science and Engineering, Koneru Lakshmaiah Educational Foundation, Vaddeswaram, Guntur District, India. **raveendrareddyy2022@gmail.com**

ABSTRACT

Numerous surveys using different techniques have been conducted in recent years to accurately classify Alzheimer's disease (AD). This research emphasized the identification of AD through neuroimaging data. However, it is important to identify symptoms as soon as possible when the disease-modifying medications function best during infection before a permanent cognitive impairment develops. The use of automated algorithms to detect the early symptom of AD to this information was very important. Machine Learning (ML) has been proposed for the evaluation of various image segmentation and database techniques. In addition, Visual Geometry Group (VGG)-16 & Improved Faster Recurrent Convolutional Neural Network (IFRCNN) method developed for the ImageNet database utilizing the mathematical model based on action recognition as a feature extractor for categorization work. Experiments are being conducted on the Alzheimer's Neuroimaging Initiative (ADNI) dataset, and the proposed system achieves the 98.32 % accuracy level *(Tab. 6, Fig. 4, Ref. 34).* Text in PDF *www.elis.sk.*

KEY WORDS: mild cognitive impairment, deep learning, Alzheimer's disease, expected risk.

Introduction

Every human being has three basic remembrances: i) working memory, which is in charge of maintaining focus and concentration while processing data; ii) short-term storage was keeping information for durations up to certain limit; iii) long-term storage should be in charge of preserving the entire occurrences researchers encounter for periods longer than days (1–3). AD was a degenerative neurological disorder that seriously affects storage, cognitive abilities, and ability to perform the simplest basic duties. Artificial Intelligence (AI) has the potential to help physicians diagnose patients faster and more accurately. This could predict the likelihood of disease at an early stage, to be prevented. Clients could apply ML to the analysis of health information and the treatment of conditions (4). However, processing clinical images may be a difficult and lengthy process.

AI devices could continually learn from experience and improve over time through ML Application. ML is the research of computer simulations that get better on their own with practice (5). ML methods develop a statistical approach that uses sample data, sometimes known as "training data," to produce predictions or decisions of specifically trained (6). ML techniques were utilized in a wide range of software, including image identification, clinical issue, and categorization if it would be difficult or impractical to perform the necessary procedures using different algorithms (7). ML is thought to be a feature of AI that imitates the human mind analyzes data and develops correlations to facilitate the decision (8). AI systems can learn unsupervised through unprocessed or unstructured information to Deep Learning (DL) is a subtype of computer vision. It is sometimes designated as a Deep Neural Network (DNN).

Every level of ML gains the ability to express the information that collects more creative and composite (9). The first representative layer in a program of image processing may extract the pixels and decode edges; the second layer may combine and encode requirements of edges; the third stage may decode a nose and eyes; the fourth layer may detect that the image comprises a face. Moreover, a DL process could determine on its own which features are best organized at which layer.

Related works

Computer-Aided Diagnostic (CAD) systems that require real-time AD diagnosis have been the subject of several investigations (10–11). They suggested categorizing the phases of AD and employed ML methods for SVM, RF, and KNN identification models (12–14). Large data sets were required to categorize and identify the representation of characteristics to avoid overflow issues. They provided in actual time the depth and transfer of learning materials in alternative ways to reach the best precision of initial AD (15). There is currently no treatment for AD using any clinical reasoning procedures, and early detection of AD is incredibly challenging, protein symptoms which are frequently utilized in AD classifications. Electroencephalogram (EEG) is a physiologi-

Department of Computer Science and Engineering, Koneru Lakshmaiah Educational Foundation, Vaddeswaram, Guntur District, India.

Address for correspondence: Raveendra REDDY, Department of Computer Science and Engineering, Koneru Lakshmaiah Educational Foundation, Vaddeswaram, Guntur District, India.

cal biomarker that has been studied extensively to identify brain damage associated with dementia (16). This method involves recording the electrical brain activity as frequency data, which is then processed to identify any anomalies in the brain (17). This method, which is based on spatial and temporal abilities can be able to detect dementia even in its early stages.

Too many variables are necessary for good multiple regression to be very accurate, increasing the complexity of implementation and reducing the reliability of conclusions. Support Vector Machines (SVM) analysis of major components, and Artificial Neural Networks (ANN) are other classifications used in the EEG. Through the skillful combination of wavelets, signal preparation methods such as non-linear science and chaos theory, and Neural Network computing a new multi-paragraph methodology for computerized EEG diagnosis of AD (18). Before applying a classification technique, mathematical markers are found with the aid of chaos theory like a mathematical microscope. In this case, the mathematical markers are used as a biomarker. The proposed multi-parameter approach has been demonstrated to significantly increase diagnostic accuracy (19).

"ML" & "DL" are comparatively new concepts were used for years in the field of medical imaging, perhaps most notably in CAD applications like "classification of breast tissue," "detection of cerebral microbleeds," "classification of brain images," and "segmentation of CT liver images" (20–22). The specific tasks such as visual recognition of objects, identification, and separation, deep CNNs are at present the most appreciated by computer vision researchers. Unlike conventional NN which receive vector input, CNNs operate on volumes, which is one of its advantages over ANNs (23). The term "parameter sharing" refers to the practice of more than one neuron in a given entity map using the same weights. Contrary to ANNs, neurons were linked; local connectivity refers to the idea that each neuron is attached to a specific section of an image.

Currently, people are building CNN from the ground up because it is uncommon to have a sizable database. Thus, the pretreatment of a CNN on a large database was typical (24). The classification method for our three-way categorization issue – MCI vs AD Cognitively Normal: should be created by domain adaptation using a cutting-edge CNN method, VGG16. The Oxford VGG has built the 16-layer network known as VGG16. It took part in the 2014 ImageNet Large Scale Visual Identification (ILSVI) ImageNet competition. One of the earliest architectures to push to 16 layers and use tiny (3x3) convolution filters to probe the depth of the network.

In this method, anomalies in the brain's shape, size, and neuronal activity are found at images of the brain. The hippocampus diminishes in size and is one of the first areas of the brain to be damaged in AD. Other areas, in particular the cerebral cortex are affected by the progression of AD (25–26). The VGG indicator of neurodegeneration is a volume measurement. It appears doubtful that only one biomarker will be found for the detection of AD alone because of the complexity of the aliment's biology and how it progresses. To enhance the precision for the detection of the aliment, the researchers hope to use a combination of biomarkers.

CNNs were a subset of CNN that should excel at detecting and classifying images, amongst other tasks. In addition, it is a variety of ANN at the Convolutional layer; independently learn the features of the image (27). In this investigation, raw images of a single front-facing camera were trained to transfer direction instructions. Finally, they concluded that CNN could identify useful road features without any explicit labeling. For their research using a graphics processing unit, they only chose 1.2 million images from the ImageNet databases, which contain images from 100 multiple categories. The highest error rate of ILSVI was 15.3 %, and they finally took first place. They suggested using CNN to categorize the Microsoft COCO object detector database and the ImageNet database. They took the lead in both the Microsoft COCO and ILSVI contests (28). The authors in (32–34) have discussed about the clinical trails of AD detection using machine learning algorithms. Compared to other classification approaches, they have the lowest failure rate for large-scale image categorization. CNN has been used in current biomedical surveys to classify images. In this study, DL was implemented using VGG16 as the basic model. In addition to the original model, additional fully connected layers were constructed as a representation of functionality.

Proposed methods

To get the best result, the preprocessed images have been improved, because different sizes could affect the classification performance of the images which were to be introduced into the CNN model were reduced to a dimension of 160 x 160. Subsequently, the flattened images that had been reformatted were saved in a matrix. Considering that the flattened format will combine all the image levels into a single layer. The images appear identical after flattering; however, there is a distinction in that the content of the image is in one layer.

The number of classes, periods, and lot sizes has been fixed at 32, 3, and 20 accordingly. The quantity of samples that would be transmitted through the system is determined by the lot size. This model forms the network from 32 training examples and then learns again from 32 examples (29). Every training sample is run once forward and once backward throughout one epoch. Here, there are 20 epochs because the definition of the number of epochs requires the realization of numerous tests of the system. The system would automatically overflow if the number of iterations would be few or many. As a result, there are 20 established periods, although this number may change as technology progresses.

Convolution operation

K(0,0) is determined using Equation (1) by first rotating Y by 180 degrees around its center component and sliding its center so that it sits on top of X.(0, 0). The next step is to multiply each reversed Y component by the X component directly below it. Various products were added together for K(0, 0). However, in the instance of IFRCNN's method, the initial stage of rotating Y by 180 degrees to the center was typically skipped, and all other phases are the same as those previously mentioned. For the above data matrices X, Y, and K procedure, which does not take into

account the inversion of the Y matrix, could be expressed mathematically as follows:

$$k(x,y) = \sum_{q=0}^{q-1} \sum_{p=0}^{p-1} I(q,p)\, \bar{J}(q-x,\, p-y) \quad (1)$$

Where, $-(S-1) \le x \le q-1, -(R-1) \le y \le p-1$, and $\bar{J}$- complex conjugation.

The main goal of introducing a level with a max-pooling procedure between each convolutional layer is to gradually lower the size of the spatial structure, or the score of h, resulting in a smaller number of variables that need to be learned and a faster network altogether. Additionally, this helps to reduce overflow (30). The most common number of K is 2, which decreases the sample size by h and by a factor of 2. The prime objective of introducing a level with a max-pooling procedure between each convolutional layer would be to gradually lower the size of the spatial structure, or the score of h, resulting in a smaller number of variables that need to be learned and a faster network altogether. In addition, it helps reduce the overflow (30). The most common number of K is 2, thus reducing the sample size by a factor of 2.

Non-linearity layers

Generally, non-linear procedures or functions—also known as activation functions – follow convolutional layers. The most popular activation features of the past were sigmoid and tanh. However, because of its shortcomings, researchers proposed other activation functions including (ReLU) & the derivatives that were favored in the majority of ML applications. The ReLU approach and its modifications are theoretically represented as follows:

$$f(i) = maximum\ (0,\ i) \quad (2)$$

$$f(i) = \begin{cases} i, & i > 0 \\ 0.01i, & otherwise \end{cases} \quad (3)$$

$$f(i) = \begin{cases} i, & i \ge 0 \\ \alpha(e^{i} - 1), & 0.01i, \ otherwise \end{cases} \quad (4)$$

In this case, Equations (2) and (3) represent Simple ReLU, Leaky ReLU, and Exponential LU. A hyper-parameter in Equation (4) could be tweaked, and its value is 0. ReLu has been demonstrated in Equation 1. It introduces nonlinearity to the network and applies pixel by pixel, substituting all negative pixels with zero.

Alzheimer classifications mathematical model

Researchers create a computing framework for AD. Figure 1 illustrates the three stages in presenting this model: data preprocessing with Freesurfer; selection based on entropy; and subsequent categorization with transfer learning.

Cortical reconstruction and volumetric separation were carried out using the FreeSurfer image assessment package that was published & publicly downloadable online, to remove extraneous information from cogitative MR images that might lead to poor learning of the categorization algorithm. In particular, recon-all autorecon1 was used, which completes only 5 of the 31 processing stages.

There are 5 methods:

1. There are different volume ratios, this procedure would group them all and offset the small movements between them.
2. Removes uneven image strength to enhance MR information.
3. At this stage in the process, the affine transformation was computed using the FreeSurfer Talairach script.
4. Adjust to accommodate changes in intensity at this point. All voxel intensities are scaled to an average white matter intensity of 110.
5. The skull is removed from the normalized image in this step.

For the categorization test, the T1-weighted MRI data of 150 participants were used, including 50 MCI, 50 CN, and 50 ADI. Table 1 provides a summary of the demographic data for the chosen gender, subjects, age, and MMSE value.

Choosing the best information could no doubt increase the likelihood that the model will succeed, even if they could utilize the 256 slices of the 150 subjects. Recent techniques assume that slices contain the majority of relevant information and choose a group randomly (31). To create slices of random, a sorting method depending on image entropy was utilized to choose the 32 data slices for each subject. The remaining slices have been removed. The image entropy of each slice has been established.

VGG16 only permits input if it has exactly 3 channels because it was developed on RGB, or 3 channels, 224x224 3 images. In addition, the height & width of the image may not be less than 48. Moreover, the images are resized to 200 x 3 which would be a good entry size for the template.

Our balanced database of 4800 images is separated between learning and testing with an 80:20 split. For three-way and two-way classes, the resulting learning and test sizes were compiled in Tables 2 and 3.

Classification using transfer learning

The IFRCNN system, VGG16 pre-trained of the ImageNet dataset was utilized to the basic structure that cogitative MRI slices could be processed to recover the attribute scores specific to that specific MRI slice. For example, we used IFRCNN to develop the classification method. Fully coupled base model levels need

Tab. 1. Demographic information.

Classification	Male Count	Females Count	Age	Age in Average	Range of MMSE value	Average range of MMSE value
Image of AD	28	26	58.33–88.95	77.12	20 – 27	22.41
Image of CN	35	19	58.29–71.35	68.19	26 – 30	27.96
Image of MCI	31	22	58.42–84.61	63.51	26 – 30	27.22

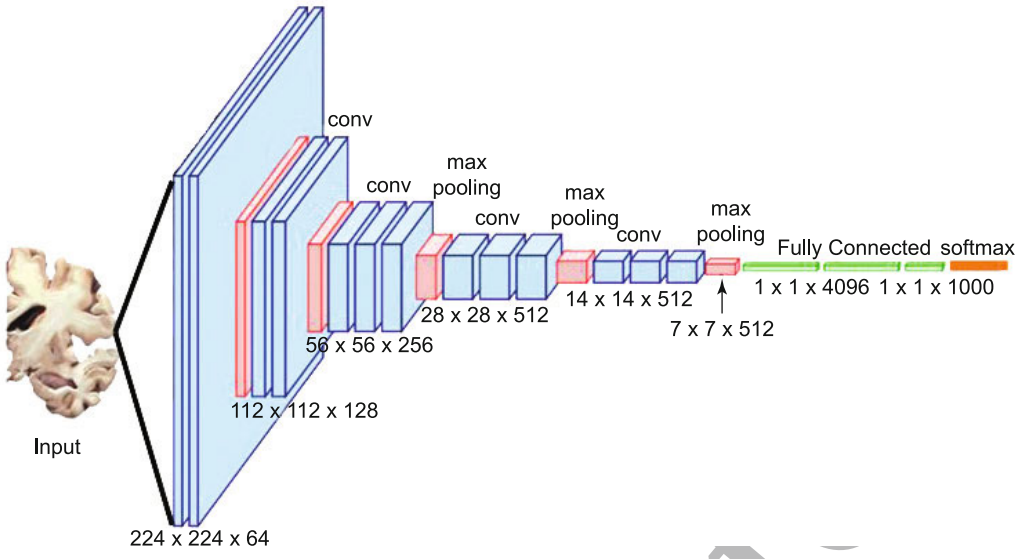

Fig. 1. ILSVI VGG16 NN structure.

Tab. 2. Three-part categorization.

Label	Size of data Trained	Size of data Tested
0 (ADI)	1282	322
1 (CN)	1282	322
2(MCI)	1282	322
Total =	3846	966

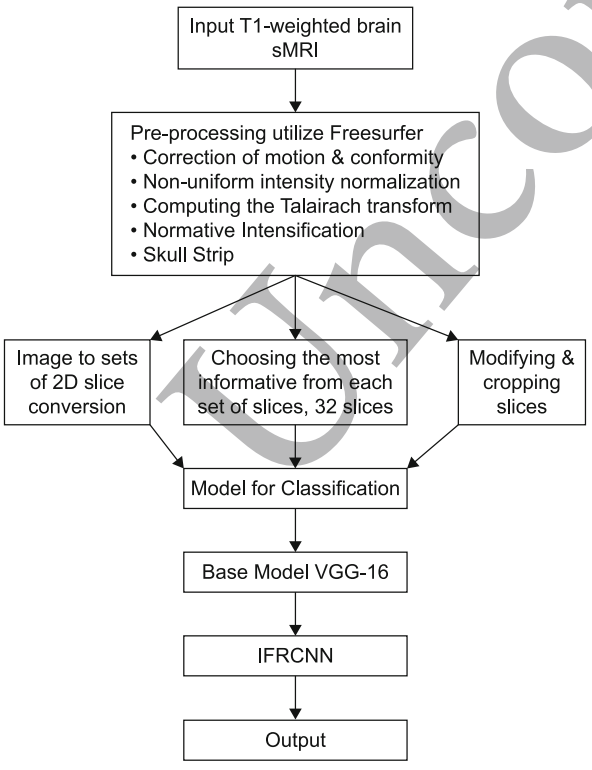

Fig. 2. Overall structure of the Work.

to be eliminated to be used for our classification assignment on ImageNet, as the outputs of these levels are 1000 category values. The output of the final convolution operation was compressed to a single size 18432 column vector after the later fully connected layers of the model were removed. New completely connected layers are generated after the previous model, the first of which has 256 neurons, the second of which has a ratio of 0.5 and is a dropout level, meaning that half of the neurons will always outcome 0, & the last of which was a softmax layer, the output is three class scores for The final categorization model for three-way categorization was shown in Figure 2.

There are over two classes, Softmax, an activation method that returns a score 0 & 1, is usually used. It is defined as:

$$f(i_x) = \frac{e^{ix}}{\sum_{y=0}^{k} e^{iy}} \tag{5}$$

The calculation of losses by categorical transversal entropy was designed to develop the method. The efficiency of a categorization algorithm outcome was a likelihood score of 0 and 1 was measured by cross-entropy, commonly known as the logarithmic reduce function. An expected output deviates from the actual time, and cross-entropy reduces and increases. The binary cross-entropy loss was computed as follows if there are 2 types:

$$L\,(j,p) = -\,(y\,\log q + (1-j)\,\log(1-q)) \tag{6}$$

RMSprop, for example, can be used to update the W variable, which corresponds to a neuron in the IFRCNN as follows:

$$R = \beta R + (1-\beta) dW^2 \tag{7}$$

$$W = W - \alpha\,\frac{dw}{\sqrt{r}} \tag{8}$$

Where, $0 \le \beta \le 1$, $dW = \frac{dL}{dW}$, and α was the learning value.

$$f(i) = maximum(0,i) \quad (9)$$

Experimental results

The subsampling layer, also known as the grouping layer, can reduce the size of each feature map while keeping the most significant feature maps. The pooling level in this case is a 2 x 2 matrix. Fully connected layers to a VGG_16 with IFRCNN used as categorization layers and subsampling and convolution layers are used to represent characteristics.

Tab. 3. Binary categorization.

Label	Size of data Trained	Size of data Tested
0 (AD and CN)	1282	322
1 (CN and MCI)	1282	322
Total	2564	644

Tab. 4. Confusion matrix.

		Predicted value		
		ADI	CN	MCI
Actual Value	ADI	292	4	28
	CN	0	320	12
	MCI	0	2	321

a) Confusion matrix of all the three category

		Predicted value	
		ADI	CN
Actual Value	ADI	318	5
	CN	1	320

b) Confusion matrix of CN and ADI

		Predicted value	
		ADI	CN
Actual Value	ADI	318	5
	CN	0	322

c) Confusion matrix of MCI and ADI

		CN	MCI
Actual Value	CN	319	4
	MCI	3	320

Tab. 5. Comparison of several image segmentation techniques.

Evaluation	Sensitivity (%)	Specificity (%)
Evaluation 1	88	94
Evaluation 2	94	97
Evaluation 3	97	99
Evaluation 4	94	97
Evaluation 5	91	96
Evaluation 6	93	97

Tab. 6. Comparison of the performance of two data sets.

Dataset	No. of images	Sensitivity (%)	Specificity (%)
Dataset 1	1618	97	99
Dataset 2	1744	94	99

Six assessment procedures were carried out in the first sub-experiment.

In evaluating the six assessment methods in the first sub-study, the period greatly strategy was chosen for the second sub-study. The second sub-experiment showed that the database would be the IFRCNN model. The results of the first sub-study make it clear that among the segmentation techniques, Evaluation 3 has the best classification performance. As a result, in the second sub-experiment, two distinct datasets were examined using this segmentation technique. The first database has 36 individuals in it. There were 1615 images after the 3D MRI movies were converted into 2D images. 1292 of these images were chosen at random to teach the proposed model. In addition, the model was tested with 323 images. In the second data set, 36 additional participants (ADI 9, NL 11, MCI 16,) are chosen. These 36 MRI methods were used to produce 1743 2D images.

A 3-channel categorization model was created using formation data of a size of 3840, in batches of 40, for 50 epochs. When the complete dataset has been transmitted back and forth over the neural network, an epoch is said to have been accomplished. In our situation, 1 period was completed in 96 stages. Each epoch stage updates the parameter values. Since accuracy was used as the primary evaluation measure, the designers defined the "measurement for evaluation" option "accuracy" in the compilation phase. It is about 10 hours to train the categorization methodology of the learning dataset and validate the testing data of time on NVIDIA Quadro K1200 GPU. The precision in Keras is calculated as follows:

$$\text{Accuracy} = \frac{\sum_{x=1}^{n} B^x}{n} \quad (10)$$

While n represents the number of examples and B^x is a Boolean variable for example x, y^x_{true} would be the real class label, and $y^x_{predicted}$ would be the correctly classified identity. It should be determined as:

$$B^x = \begin{cases} 0, y^x_{true} \neq y^x_{predicted} \\ 1, y^x_{true} = y^x_{predicted} \end{cases} \quad (11)$$

On a learning algorithm of 2560 slices, 3 more independent algorithms were also trained to provide binary classification between the 3 category AD versus CN vs MCI & AD vs MCI. The same algorithm and transfer functions were employed throughout the 50-period formation of these systems. Designs for binary categories managed to achieve 99.22 %, 99.14 %, and 99.30 %, reliability of AD vs classifications. MCI vs CN, and AD vs CN correspondingly.

Confusion matrix

Confounding matrices are created to demonstrate four types of categorization performed on the verification and test data set. The confusion matrices are described in Table 4. Using the confusion matrices presented in Table 4, they also calculated performance measures, including accuracy, recall, and F1 score, for further as-

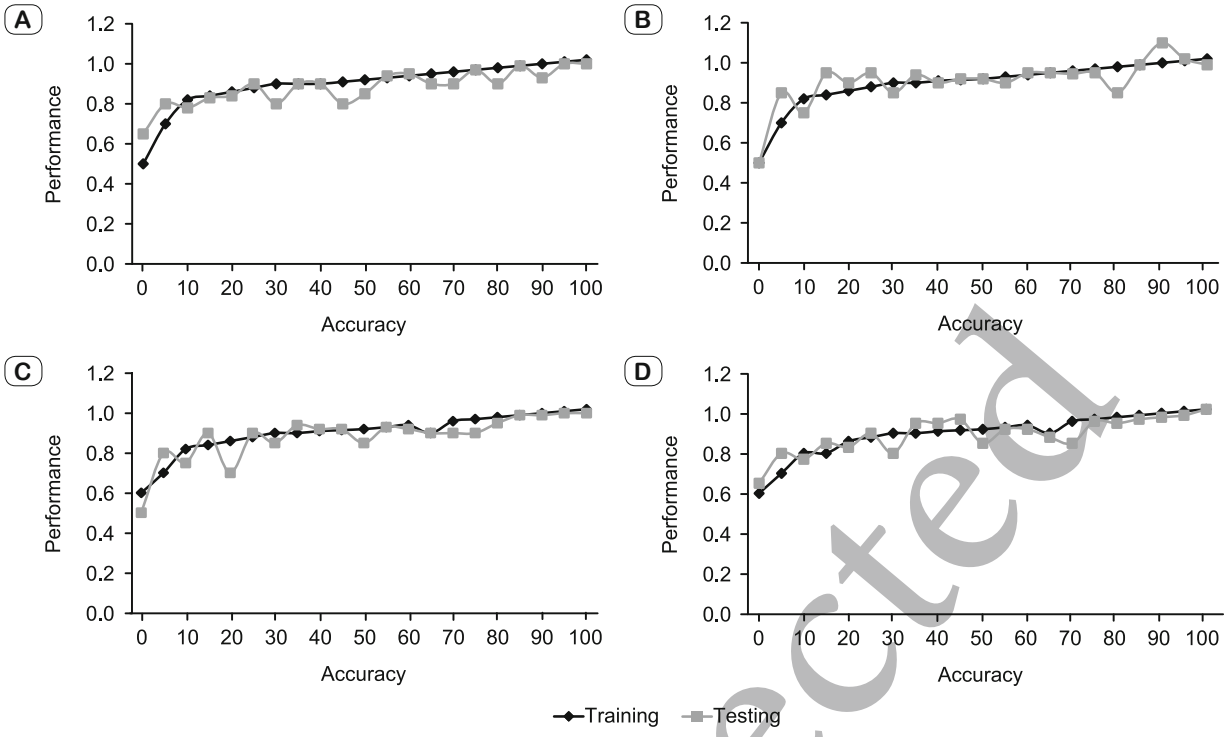

Fig. 3. Performance measures based on accuracy A) three plots (B) ADI vs CN. (C) ADI vs MCI (D) CN vs MCI.

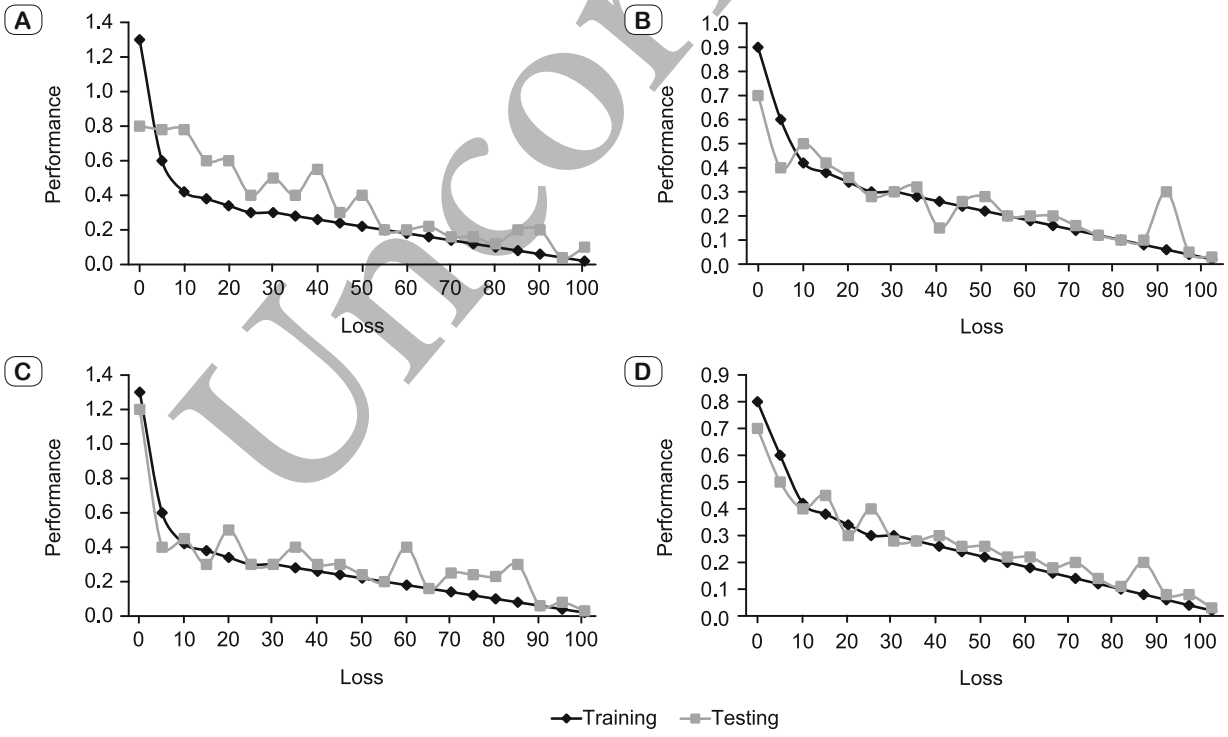

Fig. 4. Performance measures based on Loss function A) three plots (B) ADI vs CN. (C) ADI vs MCI (D) CN vs MCI.

sessment of classification techniques (Figs 3 and 4). These measures are computed as follows:

$$Precision = \frac{TP}{TP + FP} \quad (12)$$

$$Recall = \frac{TP}{TP + FP} \quad (13)$$

$$F1 = 2 \times \frac{Precision \times Recall}{Precision + Recall} \quad (14)$$

Where, for a particular classifier, FN, FP, and TP, mean False Negative, False Positive, & True Positive, correspondingly.

Confusion matrix of MCI and CN

The overall image does not provide the right classification, based on the findings from evaluations 1 and 2. The entire image is too complex compared to previous images and includes non-humid areas that are not related to ADI. These areas not covered by rain were removed from all images for which yield could be evaluated. Brain image characteristics were extracted using magnified ROI ratings 3 and 4. Enlarged ROI delivers the greater results of the 6 assessment techniques without finding edges. To emphasize the volume of the hippocampus, ventricles, and cortex, edges have to be detected. The canny edge identification method, therefore, eliminates all the white matter and grey matter information from the brain image in the enlarged ROI, which substantially reduces effectiveness when recognizing the edges. There are 2 smaller experiences in the second experience. The efficiency of various image segmentation techniques was assessed in the first sub-experiment. Table 5 provides examples of each assessment process's specificity and sensitivity.

Based on the selected restricted ROIs, evaluate items 5 and 6. The results indicate that the limited ROI offers 89 % efficiency without edge detection and approximately 92 % efficiency with edge detection. Since it concentrates more on three important characteristics than other segmentation techniques, the limited ROI should have the best accuracy, depending on the implementation assumptions. There was a conflict in the assumption that the outcomes were taken into consideration. Some major attributes are not included in the ROI, which is the fundamental drawback of the limited ROI. Two datasets were analyzed for the second subsample, and the results are presented in Table 6. The findings from the different data sets are not all that different. There's sufficient proof to show that the CNN method is independent of the database. Thus, the CNN method maintains its objectivity towards the dataset.

Conclusions

The image was complex compared to the previous images and includes rainfall-free areas that are correlated to ADI. These areas not covered by rain were then removed from all images so that efficacy could be assessed. The characteristics of the brain images were extracted using enlarged ROI evaluations 3 and 4. The ROI delivers the basic results to 6 assessment techniques with 96 % specificity and 98 % accuracy without finding an edge. In addition, the researchers suggested a transfer learning method to properly identify brain MRI sections in ADI, MCI & CN. Here they used a predefined VGG16 – IFRCNN system as a function representation for transfer learning. The researchers showed that VGG16 – IFRCNN was capable of identifying beneficial categorization challenges, even though it was instructed in relatively general images of the ImageNet dataset. As a basic model for classifier creation in future research, researchers are expected to test different neural systems of the residual network, Inception network, and the latest networks.

Reference

1. Mehmood A, Yang S, Feng Z, Wang M, Ahmad AS, Khan R et al. A transfer learning approach for early diagnosis of Alzheimer's disease on MRI images. Neuroscience 2012; 460: 43–52.

2. Naz S, Ashraf A, Zaib A. Transfer learning using freeze features for Alzheimer neurological disorder detection using ADNI dataset. Multimedia Systems 2022; 28 (1): 85–94.

3. Kantheti B, Javvaji MK. Medical Image Classification for Disease Prediction with the aid of Deep Learning approaches. In: 2022 6th International Conference on Intelligent Computing and Control Systems (ICICCS): 1442–1445).

4. Ananya PR, Pachisia V, Ushasukhanya S. Optimization of CNN in Capsule Networks for Alzheimer's Disease Prediction Using CT Images. In: Proceedings of International Conference on Deep Learning, Computing and Intelligence: 551–560).

5. Hemalatha B, Renukadevi M. Analysis of Alzheimer Disease Prediction Using Machine Learning Techniques. Information Technol Industry 2021; 9 (1): 519–525.

6. Fouladi S, Safaei AA, Arshad NI, Ebadi MJ, Ahmadian A. The use of artificial neural networks to diagnose Alzheimer's disease from brain images. Multimedia Tools Applications 2022; 1–41.

7. Khan YF, Kaushik B. Neuro-image classification for the prediction of alzheimer's disease using machine learning techniques. In: Proceedings of International Conference on Machine Intelligence and Data Science Applications, 2021: 483–493).

8. Chen X, Tang M, Liu A, Wei X. Diagnostic accuracy study of automated stratification of Alzheimer's disease and mild cognitive impairment via deep learning based on MRI. Ann Translational Med 2022; 10 (14).

9. Goenka N, Tiwari, S. Deep learning for Alzheimer prediction using brain biomarkers. Artificial Intelligence Rev 2021; 54 (7): 4827–4871.

10. Bharati S, Podder P, Thanh DNH, Prasath VB. Dementia classification using MR imaging and clinical data with voting based machine learning models. Multimedia Tools Applications 2022; 1–22.

11. Ma D, Yee E, Stocks JK, Jenkins LM, Popuri K, Chausse G et al. Blinded clinical evaluation for dementia of Alzheimer's type classification using FDG-PET: A comparison between feature-engineered and non-feature-engineered machine learning methods. J Alzheimer's Dis 2021; 80 (2): 715–726.

12. Miah Y, Prima CNE, Seema SJ, Mahmud M, Shamim Kaiser M. Performance comparison of machine learning techniques in identifying dementia from open access clinical datasets. In: Advances on Smart and Soft Computing: 79–89. Springer, Singapore.

13. Raghuvanshi A, Singh UK, Joshi C. A review of various security and privacy innovations for IoT applications in healthcare. Advanced Healthcare Systems: Empowering Physicians with IoT-Enabled Technologies 2022; 43–58.

14. Pugazhendhi LT, Kothandaraman R, Karnan B. Implementation of Visual Clustering Strategy in Self-Organizing Map for Wear Studies Samples Printed Using FDM. Traitement du Signal 2022; 39 (2).

15. Davuluri R, Rengaswamy R. Neuro-imaging-based Diagnosing System for Alzheimer's Disease Using Machine Learning Algorithms. In: Innovations in Computer Science and Engineering 2022; 501–509. Springer, Singapore.

16. Venugopalan J, Tong L, Hassanzadeh HR, Wang MD. Multimodal deep learning models for early detection of Alzheimer's disease stage. Scientific Report 2021; 11 (1): 1–13.

17. Kumari R, Nigam A, Pushkar S. An efficient combination of quadruple biomarkers in binary classification using ensemble machine learning technique for early onset of Alzheimer disease. Neural Comput Appl 2022; 1–20.

18. Khagi B, Kwon GR. 3D CNN based Alzheimer's diseases classification using segmented Grey matter extracted from whole-brain MRI. Internat J Inform Visualization 2021; 5 (2): 200–205.

19. Samhan LF, Alfarra AH, Abu-Naser SS. Classification of Alzheimer's Disease Using Convolutional Neural Networks. Internat J Acad Inform Systems Res 2022; (IJAISR): 6 (3).

20. Acharya H, Mehta R, Singh DK. Alzheimer disease classification using transfer learning. 2021; 1503–1508).

21. Alongi P, Laudicella R, Panasiti F, Stefano A, Comelli A, Giaccone P et al. Radiomics analysis of brain (18F) FDG PET/CT to predict Alzheimer's disease in patients with amyloid PET positivity: A preliminary report on the application of SPM cortical segmentation, pyradiomics and machine-learning analysis. Diagnostics 2022; 12 (4): 933.

22. Seifert R, Weber M, Kocakavuk E, Rischpler C, Kersting D. Artificial intelligence and machine learning in nuclear medicine: future perspectives. Semin Nuclear Med 2021; 51 (2): 170–177.

23. Kute SS, Shreyas Madhav AV, Kumari, S, Aswathy SU. Machine Learning–Based Disease Diagnosis and Prediction for E-Healthcare System. Adv Analyt Deep Learning Models 2022; 127–147.

24. Gharaibeh M, Almahmoud M, Ali MZ, Al-Badarneh A, El-Heis M, Abualigah L et al. Early Diagnosis of Alzheimer's Disease Using Cerebral Catheter Angiogram Neuroimaging: A Novel Model Based on Deep Learning Approaches. Big Data and Cognitive Computing 2021; 6 (1): 2.

25. Latchoumi TP, Swathi R, Vidyasri P, Balamurugan K. Develop New Algorithm to Improve Safety on WMSN. In: Health Disease Monitoring. In 2022 International Mobile and Embedded Technology Conference (MECON) 2022; 357–362.

26. Chutani G, Bohra H, Diwan D, Garg N. Improved Alzheimer Detection using Image Enhancement Techniques and Transfer Learning. In: 2022 3rd International Conference for Emerging Technology (INCET): 1–6.

27. Jyotiyana M, Kesswani N. A Study on Deep Learning in Neurodegenerative Diseases and Other Brain Disorders. Rising Threats Expert ApplSolutions 2021; 791–799.

28. Baghdadi NA, Malki A, Balaha HM, Badawy M, Elhosseini M. A3C-TL-GTO: Alzheimer Automatic Accurate Classification Using Transfer Learning and Artificial Gorilla Troops Optimizer. Sensors 2022; 22 (11): 4250.

29. Garikapati P, Balamurugan, K Latchoumi TP, Malkapuram R. A cluster-profile comparative study on machining AlSi7/63% of SiC hybrid composite using agglomerative hierarchical clustering and K-means. Silicon 2021; 13 (4): 961–972.

30. Shanmugam JV, Duraisamy B, Simon BC, Bhaskaran P. Alzheimer's disease classification using pre-trained deep networks. Biomed Signal Processing Control 2022; 71: 103217.

31. Sharma S, Gupta S, Gupta D, Altameem A, Saudagar AKJ, Poonia RC, Nayak SR. HTLML: Hybrid AI Based Model for Detection of Alzheimer's Disease. Diagnostics 2021; 12 (8): 1833.

32. Dan Pan et al. Early Detection of Alzheimers' Disease Using Magnetic Resonance Imaging: A Novel Approach Combining Convolutional Neural Networks and Ensemble Learning. Front Neurosci 2020; 14. https://doi.org/10.3389/fnins.2020.00259.

33. Jo, Taeho, Nho, Kwangsik, Saykin, Andrew J. Deep Learning in Alzheimer's Disease: Diagnostic Classification and Prognostic Prediction Using Neuroimaging Data. J Frontiers Aging Neurosci 2019. https://doi.org/10.3389/fnagi.2019.00220.

34. Battineni G, Hossain MA, Chintalapudi N, Traini E, Dhulipalla VR, Ramasamy M, Amenta F. Improved Alzheimer's Disease Detection by MRI Using Multimodal Machine Learning Algorithms. Diagnostics (Basel) 2021; 11 (11): 2103. DOI: 10.3390/diagnostics11112103.

Received November 25, 2022.
Accepted December 8, 2022.